

Effects of UV Induced-Photoaging on the Hair Follicle Cycle of C57BL6/J Mice

Xu Zhai ¹
Meihua Gong^{1,2}
Yixuan Peng¹
Daping Yang¹

¹Department of Plastic Surgery, The 2nd Hospital of Harbin Medical University, Harbin, People's Republic of China;

²Department of Plastic and Cosmetic Surgery, Shenzhen People's Hospital, Second Affiliated Hospital of Jinan University Medical College, Shenzhen, People's Republic of China

Purpose: To study the changes in the hair follicle cycle and related stem cells induced by photoaging to establish a mouse model of senescence in hair follicles.

Methods: There were 54 C57BL6/J mice randomly divided into three groups. The UVA group and the UVB group underwent photoaging induced by UV lamps for 8 weeks. Changes in skin and the hair follicle cycle were compared by physical signs, dermoscopy, and hematoxylin and eosin and Masson's staining in each group. Western blot, immunohistochemistry, and RT-qPCR were carried out to test canonical proteins and gene expression of the Wnt signaling pathway in the samples. Immunofluorescence was chosen to show variations in the stem cells related to the hair follicle cycle.

Results: There were more gray hairs in the UVA group than the other groups ($P < 0.05$). Both diameter of the hair shaft and depth of hair root were significantly decreased in the UV groups ($P < 0.05$). Stem cells and melanocytes of the hair follicles were reduced in the UVA group. UV, especially UVB, up-regulated the expression of the Wnt signaling pathway and prolonged anagen and telogen phases in the hair follicles, compared with the control group ($P < 0.05$).

Conclusion: By decreasing the number of stem cells related to hair follicles, UVA induces hair follicle photoaging characterized by hair follicle miniaturization and gray hairs. UV up-regulated the expression of the Wnt signaling pathway, and the hair follicle cycle was significantly prolonged by UVB.

Keywords: UVA, photoaging, hair follicle cycle, HFSCs, Wnt

Introduction

The history of human attempts to dye hair can be traced back to 1500 BC, and in 1860, an aromatic compound called phenylenediamine was found to show a high affinity with keratin in hair shafts.¹ Although phenylenediamine is carcinogenic, it is still used as a hair dye today. Not only is hair an important skin appendage with many physiological functions, but it is an extrinsic manifestation of fitness and social image. According to data released by the American Hair Loss Association, Americans spend US\$ 350 million on the treatment of hair loss every year,¹ which indicates the huge market. Follicular unit extraction for hair replacement has become the main procedures in our plastic surgery departments and is likely to continue to increase.

After birth, hair follicles develop and mature and are finally located in subcutaneous tissue, where they cycle through rhythmic growth and decline. There are three stages in the hair follicle cycle: anagen (growth stage), catagen (regression stage), and telogen (rest stage).² In anagen, hair follicle stem cells (HFSCs) and

Correspondence: Daping Yang
Department of Plastic Surgery, The 2nd Hospital of Harbin Medical University, Harbin, People's Republic of China
Tel/Fax +86-0451-86297062
Email dapingyang1223@hotmail.com

melanocyte stem cells (MSCs) located in the bulge region begin to proliferate because of the up-regulation of Wnt signaling pathway in the stem cell niche.^{3,4} HFSCs and MSCs migrate to the hair bulb and penetrate into subcutaneous tissue with dermal papilla (DP). During anagen, HFSCs proliferate and differentiate into keratinocytes, which enable the inner root sheath (IRS) and the hair shaft to participate in hair shaft synthesis; melanocytes generate melanin granules that are transferred to keratinocytes for hair shaft pigmentation. At the peak of anagen, the hair bulb is implanted in the subcutaneous tissue. As the hair follicle enters the catagen stage, the Wnt signaling pathway decreases and the expression of the BMP signaling pathway increases, which inhibits keratinocyte proliferation and differentiation.⁵ Apoptosis of keratinocytes in the upper part of hair follicle progresses, and the bulb migrates to the conjunction of epidermis and dermis. HFSCs and MSCs become quiescent, and hair follicles enter the telogen stage. In sum, as a vital appendant organ of skin, the growth and development of hair follicles depends on the intrinsic rhythm of HFSCs and the niche.

As the largest organ of the human body, skin has extremely important biological functions, such as conservation of water and electrolytes, immune monitoring, and temperature regulation. The skin also contains rich blood vessels, nerves, and appendages that can help the body perceive external stimuli and carry out absorption and excretion. Skin aging is caused by intrinsic and extrinsic factors; the most important extrinsic factor is photoaging.^{6,7} UV can cause multifarious pathological processes in skin. UVA (320–400 nm) promotes generation of reactive oxygen species and mediates damage to cell membranes, mitochondria, and DNA.⁸ It also up-regulates the expression of matrix metalloproteinases (MMP),⁹ as a result, the degradation of collagen is increased. UVB (280–320 nm) induces DNA damage directly when it is absorbed by the epidermis. Epidermal hyperplasia, pigmentation, and photocarcinogenesis are typical features of UVB-induced photoaging in skin. All of these changes will directly or indirectly affect the skin stem cells and their niche.¹⁰

Previous studies focused on the photoaging effects of UVB on skin,^{11,12} but little research is available on the effect of UV-induced photoaging on hair follicles. It is speculated that UVA has a greater effect on hair follicles by acting directly on the dermis. The aim of this study is to find an effective protocol for establishing a model of hair follicle aging, compare the effects of different UV

irradiation protocols on the hair follicle and HFSCs niche, and elucidate the changes of hair follicles in the process of skin photoaging.

Materials and Methods

In this study, all experiments involving animals were approved by the Medical Ethics Committee of Harbin Medical University. Meanwhile, all procedures were conducted in accordance with the Regulations on the Administration of Experimental Animals of the People's Republic of China and the ethical guidelines by the International Council for Laboratory Animal Science (ICLAS).

Experimental Animals

Two-week-old female C57BL6/J mice were purchased from the Second Hospital of Harbin Medical University and housed in the animal facility under $24 \pm 2^\circ\text{C}$ and 50% humidity. All mice were raised according to the Guidelines for Animal Experimentation of the Second Hospital of Harbin Medical University, with a 12h/12h day/night cycle. Experimental animals had food and water ad libitum.

Experimental Groups and UV Irradiation

Experimental mice were randomly divided into three groups (18 mice in each group): Control, UVB, and UVA. The hair on the dorsal skin was removed by an electric shaver every 3 days ($2 \times 2 \text{ cm}^2$ skin exposure). Mice in the control group were only shaved and there was no irradiation. The UVB group were exposed under a narrow spectrum UVB lamp (wavelength 290–320 nm, peak wavelength 312 nm, TL20W; Philips, The Netherlands). The UVA group were exposed under a narrow spectrum UVA lamp (wavelength 340–370 nm, peak wavelength 365 nm, TL-D/18W; Philips, The Netherlands). Mice of each group were placed in a closed box and could move freely during exposure. The UV lamp was 25 cm from the bottom of the box. Mice in the UVB group were exposed for 15 min (1 minimal erythemal dose, MED) each day; in the UVA group, the time of exposure was 20 minutes (1 MED) each day, five times per week in the first week. During the 2nd to 8th week, each group received 2 MED three times per week.^{10,13}

Hair Follicle Cycle and Gray Hair

The 2-week-old mice had just gone through the first hair follicle cycle, and all hair follicles were in telogen. When

the mice hair follicles entered anagen, the skin on their backs gradually turned gray. The duration of the second anagen and telogen were recorded. After 8 weeks of UV irradiation, $1 \times 1 \text{ cm}^2$ skin in the dorsal irradiation area was selected to count the number of gray hairs.

Symptoms of Photoaging Skin and Specimen Harvest

The changes of skin and hair growth in anagen, catagen, and telogen phases in mice were recorded, and aging damage such as wrinkles, pigmentation, and erythema were observed by dermoscopy. All tissue harvest procedures were carried out under sevoflurane (Hengrui Medicine Co., Jiangsu, China) anesthesia and the animals were executed by CO_2 asphyxiation. At the 8th week, skin samples $1 \times 1 \text{ cm}^2$ were cut within 0.5 cm from the edge of the shaved area on the mice dorsum for relevant experimental examination. Skin samples of each group were put in nitrogen to extract protein and mRNA ($n=6$). Skin samples of each group were placed in 4% formaldehyde solution for hematoxylin and eosin (H&E), Masson's trichrome, immunohistochemistry (IHC), and immunofluorescence (IF) staining ($n=6$).

H&E Staining and Masson's Trichrome Staining

Changes in skin epidermal thickness, hair follicle depth, diameter of hair shaft, and hair follicle density were assessed via H&E staining. Data acquisition included mean values of five random areas in the same section. Masson's trichrome staining was chosen for collagen density comparison. All skin samples were embedded in a paraffin embedded machine (HD-310, Hubei, China), sliced by paraffin section machine (Thermo, England), and observed by advanced analysis inverted microscope (Nikon, Japan).

IHC and IF Staining

IHC was carried out using antibodies against Wnt10b (1:200; ab70816; Abcam, USA), β -Catenin (1:100; #8480; CST, USA), and LEF1 (1:100; ab137872; Abcam, USA) to locate and investigate changes of proteins in the Wnt signaling pathway in the sections. Skin samples were cut into $4\text{-}\mu\text{m}$ sections, followed by 3% hydrogen peroxide incubation for 10 min. Then, slices were soaked in PBST for 3 minutes before being blocked with 3% BSA. Primary rabbit antibodies were incubated

at 4°C overnight. After three washes with PBST, sections for IHC were incubated with the secondary antibody, horseradish peroxidase- (HRP) labeled goat anti-rabbit IgG (PV-6001; ZSGB-BIO, China), for 1 hour at 37°C . After these procedures, slices were blocked with neutral resin and analyzed by inverted microscope. Area and optical density (OD) were measured by ImageJ. Average optical density (AOD) = OD/area.

IF was carried out using anti-Sox9 (1:600; #82630; CST, USA) as the first primary antibody, anti-Ki67 (1:200; ab16667; Abcam, USA) or anti-tyrosinase (1:100; ab180753; Abcam, USA) as the second primary antibody, and DAPI (abs50012; Absin, China) to label HFSCs and hair-follicle-related cells. After the same protocol for IHC antibody incubation, sections were incubated with monochromatic fluorescent dyes 520. There was 15-min microwave antigen repair after PBST washes, and then the next primary antibody was incubated. The procedure was repeated with incubation with monochromatic fluorescent dyes 570. Finally, DAPI was stained. All IF steps were followed according to the instructions of the multiple fluorescent immunohistochemical staining kit (abs50012; Absin, China).

Western Blot

Protein levels of Wnt10b, β -catenin, LEF1, and tyrosinase (Tyr) in the dorsal skin were analyzed by Western blot. Proteins were extracted from skin samples which were lysed by RIPA and PMSF (100:1) buffer at 4°C . After centrifugation at $16000g$ for 10 min, supernatant was collected. Then proteins were separated using 10% sodium dodecyl sulfate-polyacrylamide gel electrophoresis (SDS-PAGE) for 2 hr and transferred to a polyvinylidene fluoride (PVDF) membrane for 20 min at 20 V. Membranes were incubated separately overnight at 4°C with the primary rabbit antibody: anti-Wnt10b (1:500; ab70816; Abcam, USA), anti- β -catenin (1:1000; #8480; CST, USA), anti-LEF1 (1:1000; ab137872; Abcam, USA), anti-Tyr (1:500; ab180753; Abcam) and anti-GAPDH (1:5000; 10494-1-AP; Proteintech, China) as a control. After washing three times, the membranes were incubated with peroxidase-conjugated goat anti-rabbit IgG (1:5000; ZB2301; ZSGB-BIO, China) at 24°C for 1 hr. The membrane blots were visualized with an enhanced luminol chemiluminescent (ECL) kit (HaiGene, China) after washing three times.

Real-Time Quantitative Polymerase Chain Reaction

After extracting with TRIzol reagent (Roche, Switzerland), mRNA was quantified by spectrophotometry. Primers were designed and synthesized corresponding to data in GenBank (Table 1). Expressions of Wnt10b, β -catenin, LEF1, c-Myc, CCND1, and Fos genes were tested using an ABSscript II One Step SYBR Green RT-qPCR Kit (ABclonal; Wuhan, China). The program was set as 42°C for 5 min and 95°C for 1 min, followed by 40 cycles of 95°C for 5 sec and 60°C for 34 sec.

Statistical Analysis

All experiments were performed three times. All data were presented as mean \pm SD. If the ANOVA showed differences, Dunnett's test was used between the experimental groups and the control group. If $P < 0.05$, results were considered statistically significant.

Results

Phenotypes of Photoaging Skin Related to UV Wavelength

Erythema could be seen on the dorsum of the irradiated mice (Figure 1A and D). The epidermis of the UVB

group was exfoliated clearly at 72 hr (Figure 1A). After irradiation for 4 wk, abnormal pigmentation was observed in the UVA group (Figure 1E). In the UVB group, the pigmentation was more uniform, accompanied by a large amount of epidermal hyperplasia and exfoliation (Figure 1B). At the end of the 8th week of irradiation, the skin of the UVB group became thicker and coarse, accompanied by deeper and wider wrinkles (Figure 1C). Meanwhile, H&E staining showed that there was no significant difference between the UVA group and the control group with respect to epidermal thickness (Figures 2A, C and 3E). Compared with the other two groups, the proliferation of keratinocytes in the UVB group was abnormal, disordered and multi-layered (Figure 2B and E, \downarrow); the epidermis was clearly exfoliated (Figure 2E, \leftarrow); the thickness increased significantly (Figures 2B and E, \downarrow and 3E).

Masson's staining was used to show the collagen of the dermis. Compared with the control group (Figure 2D), collagen in the irradiated groups was disordered and degraded (Figure 2E and F, \blacktriangle). In the UVB group, hyperplasia of sebaceous glands could be seen, reflecting the characteristic dermal changes of skin photoaging (Figure 2E, \oplus).

UVB Prolongs the Hair Follicle Cycle

The skin of the C57BL6/J mice showed different colors because of the different phases of the hair follicle cycle. The skin on the dorsum of the C57BL6/J mice gradually changed from pink to black in anagen and from black to gray in catagen, and then to pink in telogen. Therefore, the duration of each phase could be measured according to the skin exposure area of experimental mice. Compared with the control group, anagen in the UVB group was significantly prolonged ($P < 0.05$), but there was no statistical difference in the UVA group. The UVB group was also prolonged in telogen ($P < 0.05$) (Figure 3A).

UV Up-Regulates the Expression of the Wnt Signaling Pathway in Hair Follicles

Keratinocytes expressed Wnt10b, β -catenin, and LEF1 in the DP and IRS in IHC staining slices (Figure 4). The expression of Wnt10b, β -catenin, and LEF1 in UVB, UVA, and control groups decreased in turn by average optical density (AOD) analysis (Figure 4B–D).

Table 1 Sequences of the Primers for RT-qPCR

c-Myc-F	TGGAACGTCAGAGGAGGAC
c-Myc-R	TGTGCTCGTCTGCTTGAATG
CCND1-F	GCGTACCCTGACACCAATCTC
CCND1-R	ACTTGAAGTAAGATACGGAGGGC
Wnt10b-F	GCGGGTCTCCTGTTCTTGG
Wnt10b-R	CCGGGAAGTTAAGGCCAG
β -Catenin-F	TATGGACTGCCTGTTGTGGT
β -Catenin-R	TCGTGGAATAGCACCTGTT
LEF1-F	AGAGCGAATGTCGTAGCTGA
LEF1-R	GCTGCATGTGTAGCTGTCTC
Fos-F	CGGGTTTCAACGCCGACTA
Fos-R	TGGCACTAGAGACGGACAGAT
GAPDH-F	GGTGAAGGTCGGTGTGAACG
GAPDH-R	CTCGCTCCTGGAAGATGGTG

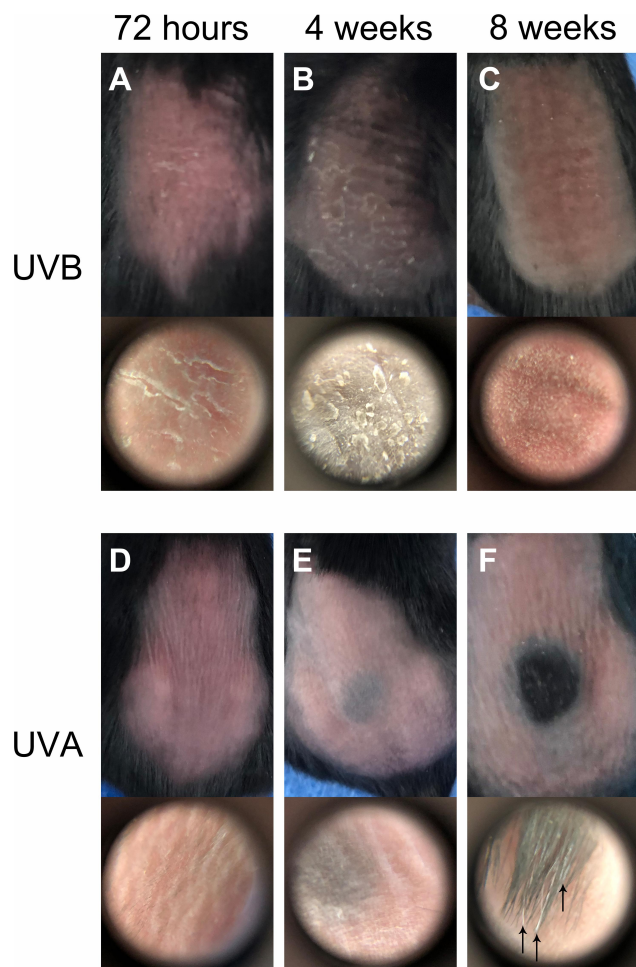


Figure 1 Skin damage by UV irradiation. (A–C) At 72 hr after 1 minimal erythemal dose (MED) irradiation of UVB, epidermal exfoliation could be found on the dorsum of C57BL/6J mice and clearly shown by dermoscopy (60x). During anagen, the dorsum of mice was black and the exfoliation of epidermis was more serious in the UVB group in the 4th week. There were heavy wrinkles on the dorsum of mice, and the photoaging skin was tanned and coarse by the 8th week. (D–F) Erythema was the striking feature of skin on the dorsum of mice in the UVA group. After 4 weeks' irradiation, pigmentation formed on the back of mice. In addition, there were more grey hairs in the experimental region of the UVA group in the 8th week ($P<0.01$).

Western blot showed that the expression of Wnt10b and β -catenin in the UVA and UVB groups was significantly higher than in the control group ($P<0.01$) (Figure 5A–C), the expression of LEF1 in the UVA group was statistically higher than in the control group ($P<0.05$), and the expression of LEF1 in the UVB group was significantly higher than in the control group ($P<0.01$) (Figure 5A and D).

Furthermore, to compare the expression of the Wnt signaling pathway between the UVA group and the UVB group, we tested expressions of genes related to the Wnt signaling pathway by RT-qPCR. Compared with the control group, relative mRNA expressions of Wnt10b, β -

catenin, and LEF1 in the UVB group were significantly increased ($P<0.01$) (Figure 6A–C). Relative mRNA expressions of β -catenin and LEF1 in the UVA group were statistically higher than in the control group ($P<0.05$) (Figure 6B and C). C-Myc, which are the downstream target genes of the Wnt signaling pathway, were significantly increased in the UVB group ($P<0.01$) and UVA group ($P<0.05$) (Figure 6D). CCND1, which encodes cyclin D1, is also regulated by the Wnt signaling pathway. Fos, which encodes the leucine zipper protein, plays an important role in the synthesis of activator protein-1 (AP-1). Both cyclin D1 and AP-1 are key regulators of proliferation and differentiation. CCND1 and Fos were statistically increased in the UVB group ($P<0.05$) (Figure 6E and F).

UVA-Induced Degression of Transit-Amplifying Cells and Melanocytes in Hair Follicles and Increased Gray Hair

The result of gray hairs in the 1×1 cm² samples showed that UVA significantly increased unpigmented hairs ($P<0.01$) (Figures 1F and 3B). Gray hairs in the UVB group were statistically significantly fewer than in the control group ($P<0.05$) (Figure 3B). Levels of Tyr were tested by Western blot. Interestingly, in the UVA group, the expression of Tyr was significantly higher than in the control group ($P<0.01$), and Tyr expression in the UVB group was also increased ($P<0.05$) (Figure 5A and E). Therefore, multiple IF staining was used to localize HFSCs and melanocytes. Significantly Sox9-positive HFSCs were observed in the bulge region and outer root sheath (ORS) in the UVA group than in the other groups. Ki67-positive cells were concentrated in the hair bulbs (Figure 7).

Tyr-positive melanocytes were found mainly in the bulge region and IRS of the UVB group and the control group, but in the UVA group, the Tyr-positive melanocytes were mainly distributed in the epidermis. UVA-induced HFSCs and MSCs decreased and there was stemness deprivation (Figure 8).

UVA-Induced Hair Follicle Miniaturization is More Effective for C57BL/6J Mouse Hair Follicle Aging Model Establishment

Although by coronal skin section we found that there were no statistically significant differences in hair follicle

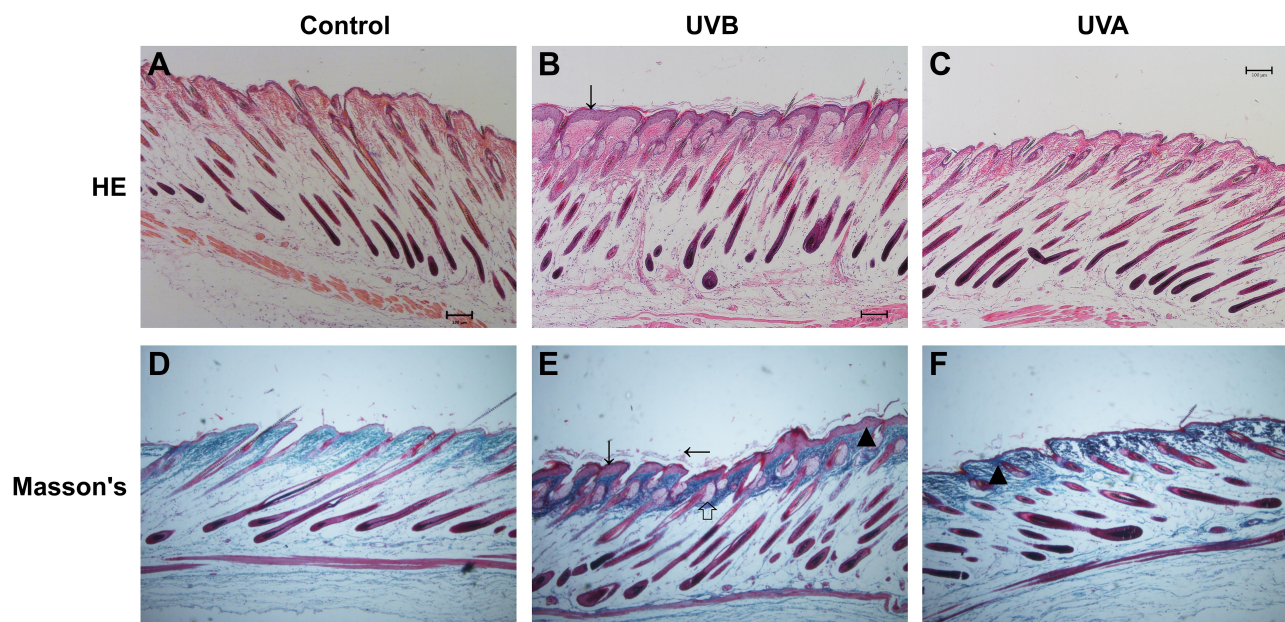


Figure 2 H&E and Masson's staining (4x). Skin changes in histology. There was no statistical difference in epidermis between the control group and the UVA group (**A, D, C** and **F**). In the UVB group, the epidermis was significantly increased (**B** and **E, ↓**). There were large amounts of exfoliated epidermis in the UVB group (**E, ←**), and it was easy to see the hyperplastic sebaceous glands (**E, ←**). In the UV irradiation group, the collagen in dermis was disordered and the degradation was increased (**E** and **F, ▲**).

number among groups, compared with the control group, the diameter of hair shafts was significantly decreased in both the UVA and the UVB groups ($P < 0.01$) (**Figure 3C**). The depth of hair roots was statistically less in the UVA group ($P < 0.05$) and in the UVB group ($P < 0.01$) (**Figure 3D**). Combined with the increase of gray hair, it was obvious that UVA induced greater hair follicle senescence than UVB did.

Discussion

Self-renewal and pluripotency are characteristics of stem cells (SCs). SCs equilibrium is maintained through asymmetric divisions.¹⁴ When activated by a signal, SCs divide into two progeny cells, and this division is different between protein and mRNA. Subsequently, extracellular signal-mediated integrin synthesis changes, and one progeny cell leaves the SCs niche and becomes a transit-amplifying cell (TA cell), while the other offspring cell left in the niche retains all the genetic characteristics of the progenitor stem cell. By asymmetric division, SCs could avoid being stimulated by physical and chemical factors in a different environment, as well as avoid DNA mismatching caused by frequent replication, to maintain the stability of their genetic traits. After three to four generations of proliferation, TA cells differentiate into mature cells. Therefore, according to the different functions of organs or tissues, the metabolic renewal ratio of cells is different,

which determines the frequency of the SCs cycle. The anagen phase of normal human hair is 2–7 years;¹⁵ about 85% of the scalp hair follicles are in anagen at any point in time.¹ This growth rate requires a large number of TA cells to supplement the apoptotic root sheath cells.

A hair follicle is a cycling organ with dynamic growth. The activation of stem cells in the bulge region is the basis of hair growth. Studies^{16,17} have proved that HFSCs have the ability to differentiate into fat, bone, muscle, and cartilage tissues. Through in vitro and in vivo experiments, Lako et al¹⁸ found that HFSCs have the ability to differentiate into hematopoietic cells, which can help improve the hematopoietic function of mice. Nestin-positive HFSCs can differentiate into neuron cells, neuroglia cells, or Schwann cells under different induction conditions and can be used to repair nerve injury.^{19,20} Other than providing various physiological functions for hair, HFSCs, as an important component of skin stem cells, play an important role in wound healing, skin homeostasis, and tumorigenesis.^{21–23}

In Sox9-knockout mice, hair shaft fragility increased and atrophied; hair bulb stromal cells decreased and the HFSCs in the bulge region decreased.²⁴ In this study, Sox9 was labeled for HFSCs, and Ki67 was labeled for TA cells in hair follicles. IF staining showed that Sox9-positive cells distributed along the ORS of hair follicles and Ki67-positive cells were located in the bulbs. The numbers of Sox9-positive cells and Ki67-positive TA cells in the UVA

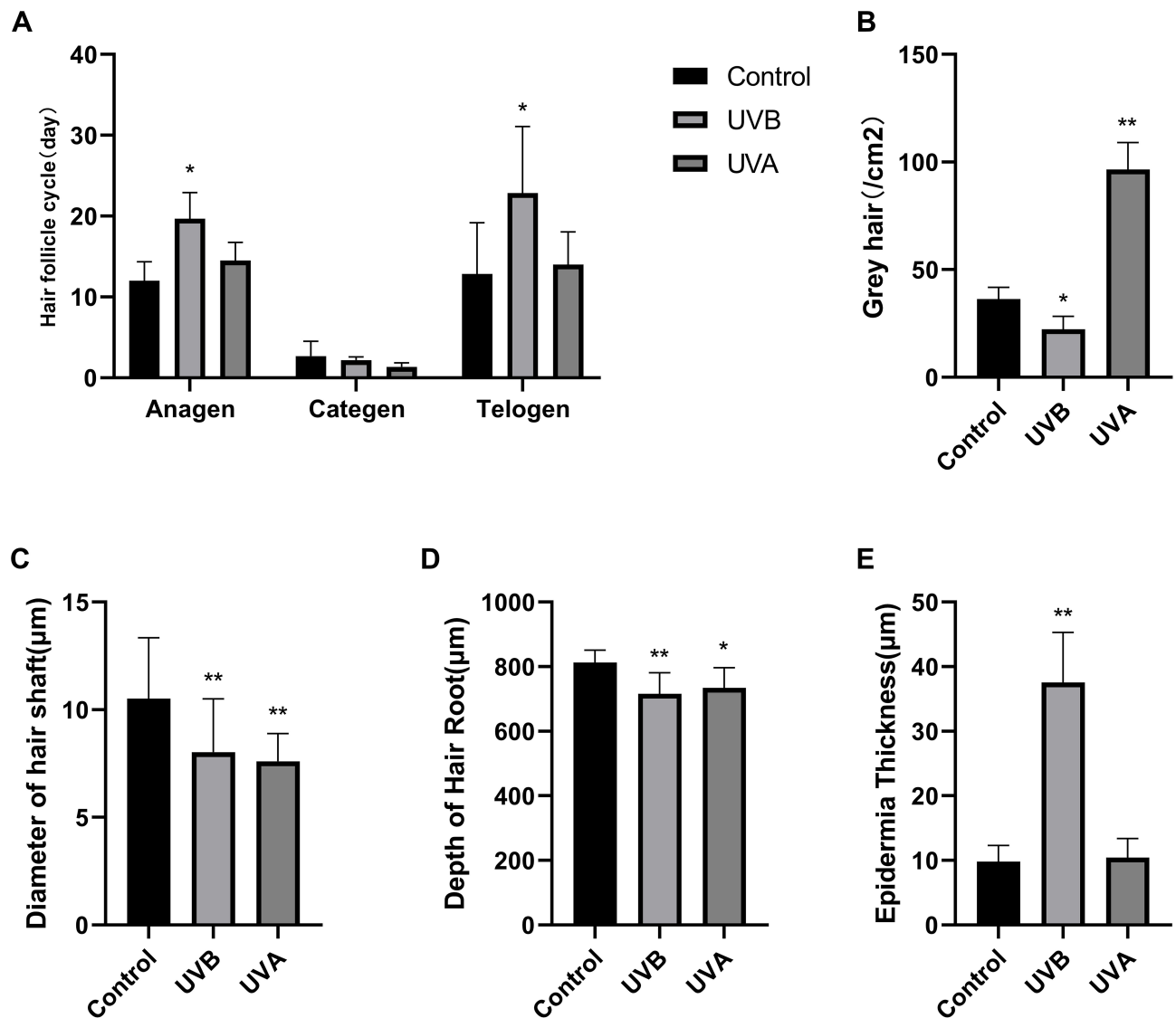


Figure 3 (A) Compared with the control group, the anagen and telogen phases of hair follicles were statistically prolonged in mice in the UVB group, and there was no significant difference in the UVA group. (B) There were more grey hairs in the UVA group. However, in the UVB group, there were fewer grey hairs compared with the control group. (C) The diameter of hair follicles in both the UVB group and the UVA group was significantly less than in the control group. (D) The depth of hair root was significantly decreased in the UVB and in the UVA groups. (E) Compared with the control group, the thickness of epidermis was significantly increased in the UVB group. (* $P < 0.05$, ** $P < 0.01$).

group were significantly lower than in the other two groups. In contrast to the up-regulation of the Wnt signaling pathway, the UVA group may have more damage to stem cells than the other groups. The regeneration of tissue cells depends not only on the strong proliferation and differentiation ability of SCs but also on the interaction between cells. Different signaling pathways affect the biological activity of the stem-cell niche. Studies^{25–28} have shown that the signaling pathways related to hair follicle growth and development mainly include Wnt/ β -catenin, TGF- β /BMP, Notch, sonic hedgehog, and other related signaling pathways.

The canonical Wnt signaling pathway plays an important role in hair follicle embryogenesis, cycle regulation, and hair pigmentation.^{4,25} When hair follicles enter anagen, Wnt signaling pathway ligands bind and activate receptors in the cell membrane, causing accumulation of β -catenin in cytoplasm, which is transported to the nucleus. β -catenin up-regulated the expression of LEF/TCF, which increased the expression of downstream genes c-Myc, cyclin D1, and Runx1, activating proliferation and differentiation.²⁵ At the same time, it was found that the expression of Wnt suppressor genes related to the bulge region was significantly inhibited, which was

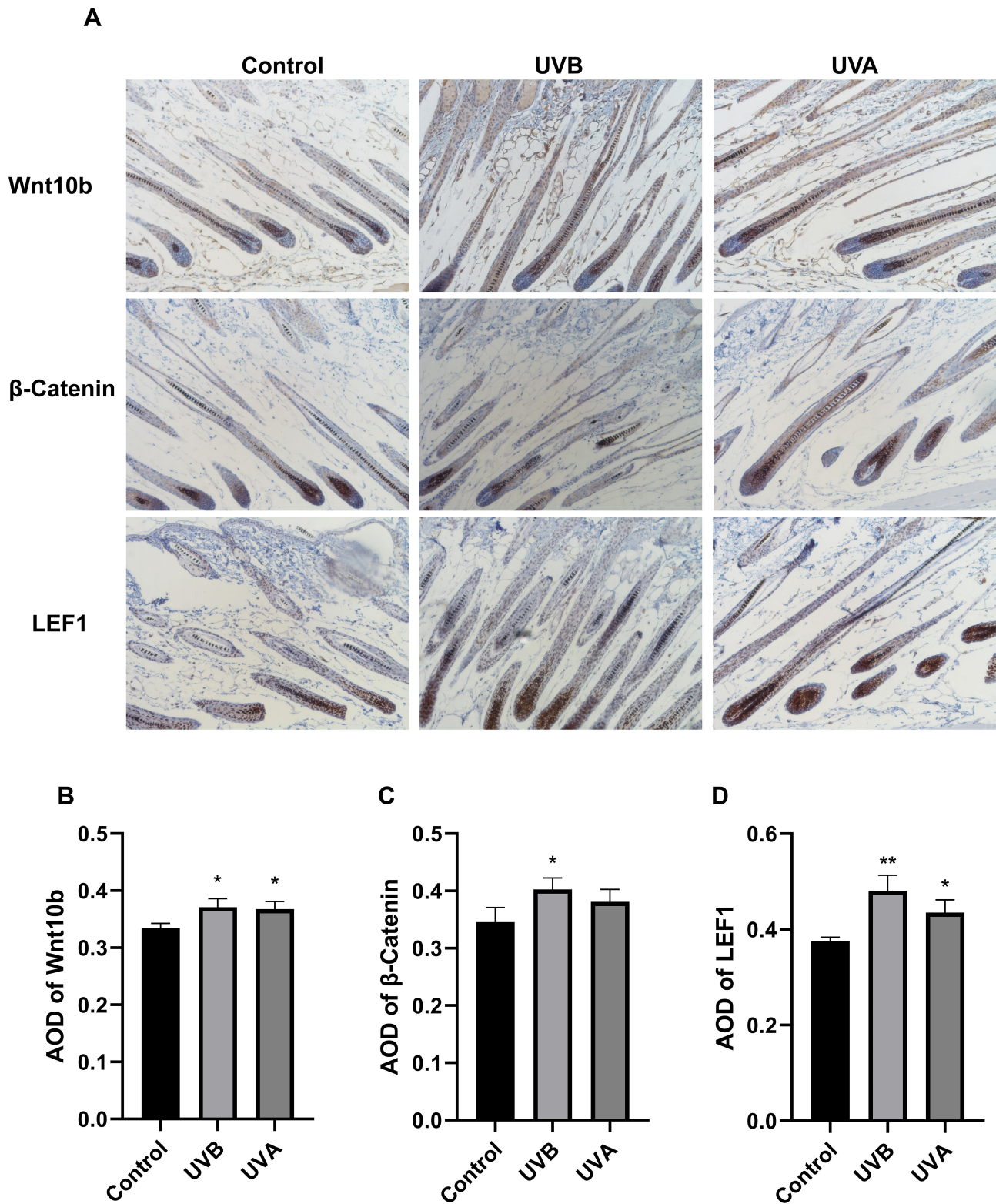


Figure 4 Immunohistochemistry (IHC) for proteins in the Wnt signaling pathway. **(A)** During anagen, the Wnt signaling pathway-related proteins, such as Wnt10b, β -catenin, and LEF1 were highly expressed in the IRS of hair follicles. **(B)** The expression of Wnt10b in hair follicles of the UV group was higher than in the control group. **(C)** The expression of β -catenin in hair follicles of the UVB group was higher than the control group, but there was no statistical difference between the UVA group and the control group. **(D)** The expression of LEF1 in hair follicles of the UVB group was significantly increased compared to the control group, and the protein in hair follicles of the UVA group was also higher than in the control group. (* $P < 0.05$, ** $P < 0.01$).

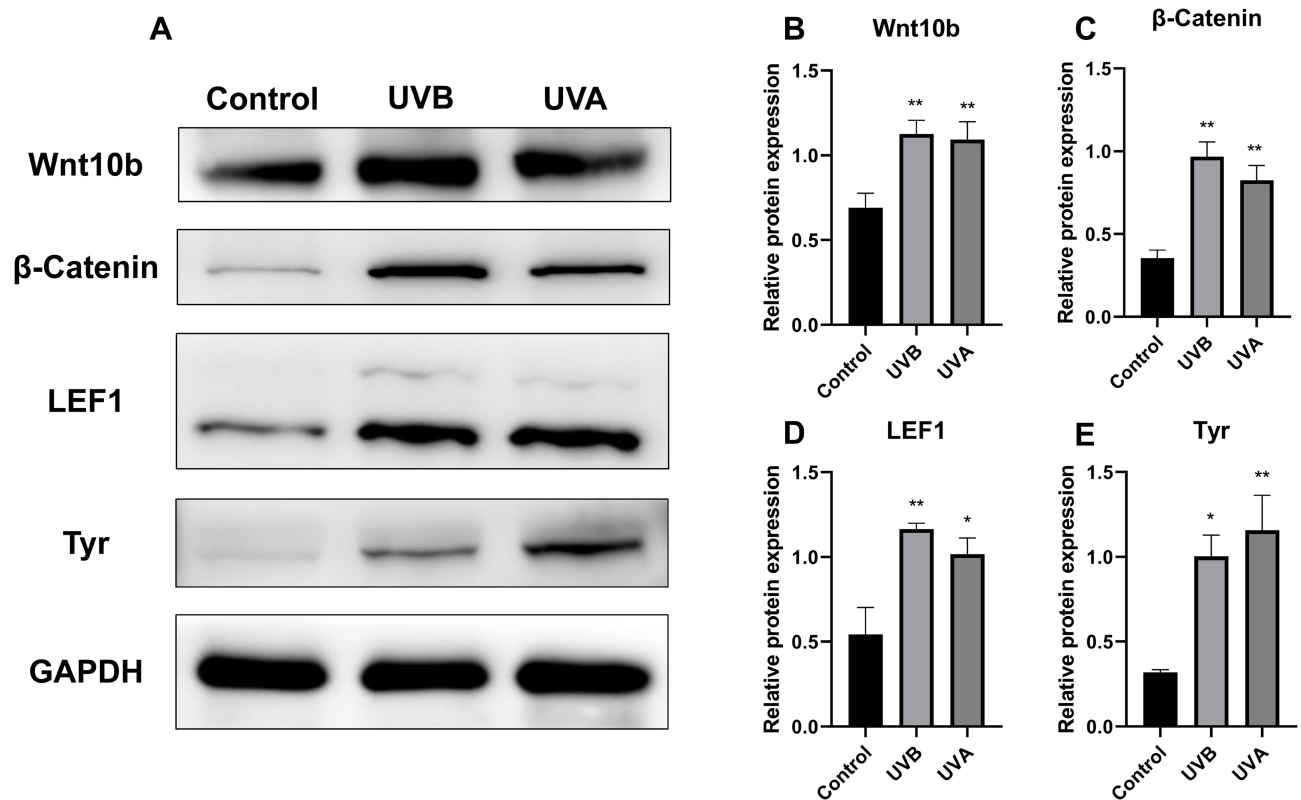


Figure 5 Relative protein expression by Western blot. **(A and B)** Compared with the control group, relative protein expression of Wnt10b was increased in both the UVB and the UVA groups. **(A and C)** The expression of β -catenin was also higher in both the UVB and the UVA groups as compared to the control group. **(A and D)** LEF1 expression was higher in the UVB and UVA groups than in the control group. **(A and E)** Western blot showed that UV irradiation up-regulated the expression of Tyr. (* $P < 0.05$, ** $P < 0.01$).

confirmed in human and mouse hair follicles, and the expression of related inhibitors such as *srfp1*, *DAB2* and *TCF3* was down-regulated.²⁹

Through the localization and quantitative detection of Wnt signaling pathway-related proteins in hair follicles, it was found that UV up-regulated the expression of the Wnt signaling pathway in hair follicles, thus prolonging anagen, especially in the UVB group. This may be due to wavelength dependence; UVB mainly acts on the epidermis, causing the proliferation of keratinocytes. The ORS of the hair follicle is connected with the epidermis, and stem cells in the niche are regulated by similar signals. The up-regulated expression of the Wnt signaling pathway leads to the proliferation of epidermal keratinocytes and the thickening of the epidermis, the proliferation of hair follicle epithelial keratinocytes, the prolongation of hair follicle anagen, and the increase of hair shaft growth. All of these can reduce the damage to tissue caused by UV. The specific mechanism needs further study.

There have been some clinical trials on UV irradiation for skin disease. The primary mechanism of UV therapy

was to promote the proliferation and differentiation of epidermal cells and melanocytes by up-regulation of the Wnt signaling pathway.^{30,31} In addition, epithelial Wnt ligand secretion could promote hair follicle growth and regeneration.²⁵ In this study, the up-regulation of the Wnt signaling pathway was also observed after UV irradiation. However, in another in vitro study, the reduction of hair shaft elongation, premature catagen entry, and reduced hair matrix keratinocyte proliferation were observed in UV-irradiated hair follicles.³² UVA could directly injury hair follicles in the dermis because of its longer wavelength. There was a reduction of Sox-9-positive cells and Ki67-positive cells in the hair follicles of the UVA group. As a result, the up-regulation of the Wnt signaling pathway did not prolong the anagen phase in hair follicles.

Senility in hair was characterized by hair follicle miniaturization and gray hair.^{33,34} In this study, both depth of hair root and diameter of hair shaft in UV groups were statistically decreased compared with the control group ($P < 0.05$), in particular, gray hairs in the UVA group of

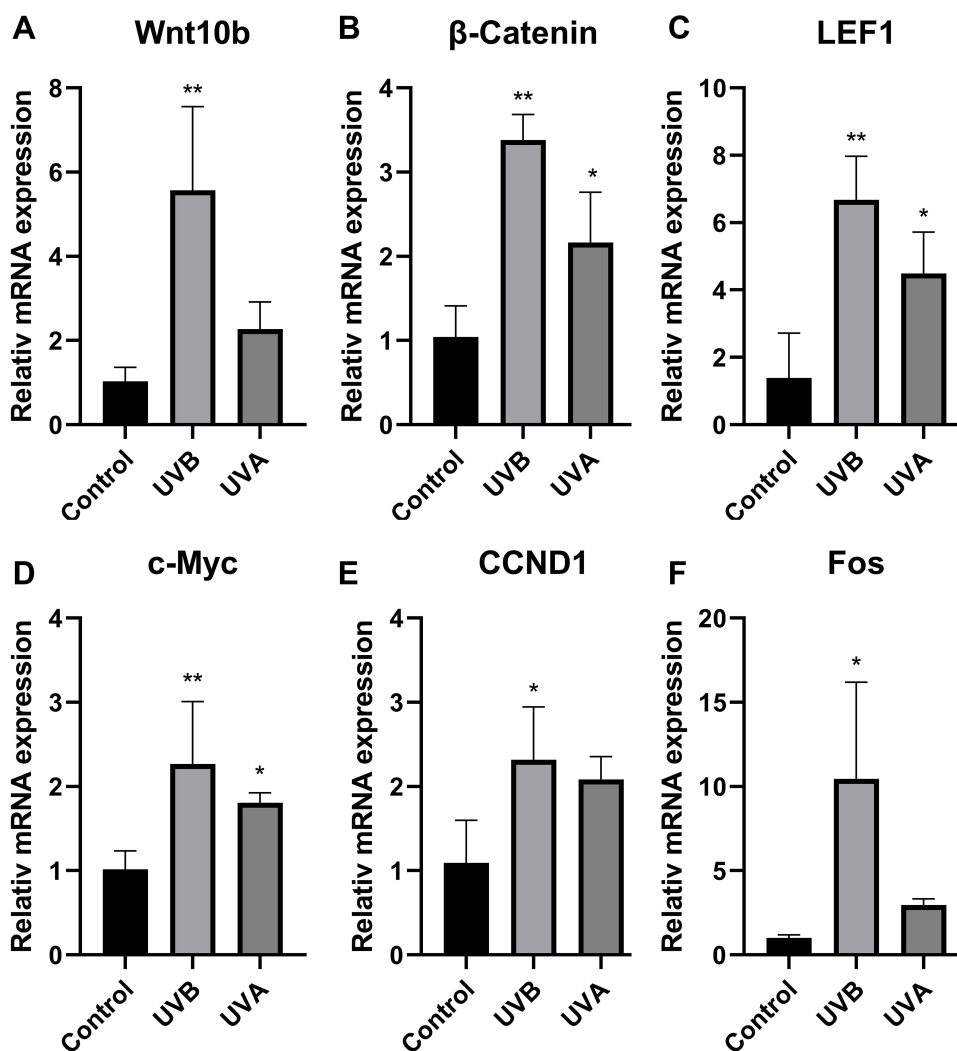


Figure 6 (A) UVB up-regulated the expression of Wnt10b. (B) Both UVB and UVA could up-regulate the expression of β -catenin, and the expression was especially higher in the UVB group. (C) The expression of LEF1 could be up-regulated by UV irradiation, especially UVB. (D) C-Myc, the downstream gene of the Wnt signaling pathway, was significantly up-regulated by UVB. The expression of c-Myc in the UVA group was statistically higher than in the control group. (E) UVB up-regulated the expression of CCND1. (F) UVB up-regulated the expression of Fos. (* $P < 0.05$, ** $P < 0.01$).

mice increased significantly ($P < 0.01$). Senescent phenotype was obvious in hair follicles. In the UVA group, as a consequence of HFSCs losing stemness or degeneration from photoaging, insufficient TA cells were generated during anagen, which eventually causes hair follicle miniaturization. Furthermore, the decrease of MSCs directly led to the decrease of melanocytes in hair follicles and gray hairs.

In the other hand, according to the different signs in skin after UV irradiation, Sachs³⁵ divided photoaging skin into two clinical types: atrophic skin photodamage and hypertrophic skin photodamage; the former was susceptible to skin carcinoma. In this study, mice in the UVA group showed atrophic skin photodamage: fine wrinkles,

erythema, and telangiectasia. UVB induced hypertrophic skin photodamage, and the skin in C57BL/6/J mice featured coarse and prominent wrinkles. This means that the clinical type of photodamage is determined not only by race or genetic characteristics but also is closely related to UV wavelength. Although the Wnt signaling pathway plays an important role in tumorigenesis, expression levels of related genes did not show an obvious increase in the UVA group, as compared with the UVB group. Fos represses p53 expression, thereby enabling tumor development.³⁶ In patients with senescent alopecia, there was a significantly decreased expression of Fos.³⁷ Because of its important role in aging and tumorigenesis, Fos expression was examined by RT-qPCR in this study. The

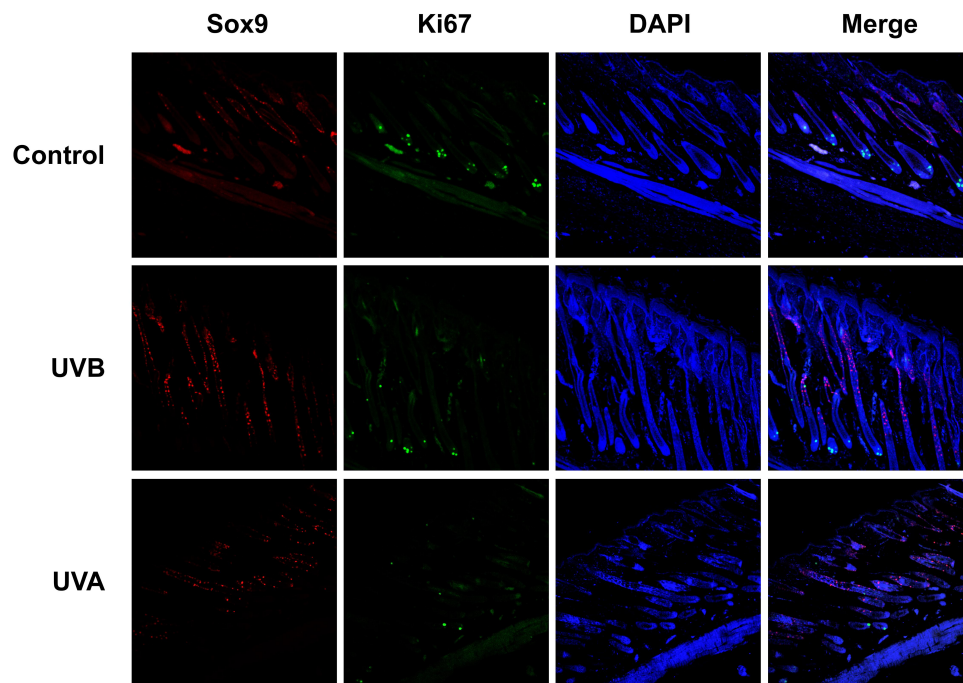


Figure 7 Hair follicle stem cells (HFSCs) and transit-amplifying (TA) cells in the three groups. Red fluorescence was chosen to label Sox9-positive cells which were HFSCs; the Sox9-positive cells were located in outer root sheath (ORS) of hair follicles. Ki67-positive cells labelled by green fluorescence were located in the hair bulbs. Merged fluorescence images showed that there were decreases of HFSCs and TA cells in the UVA group.

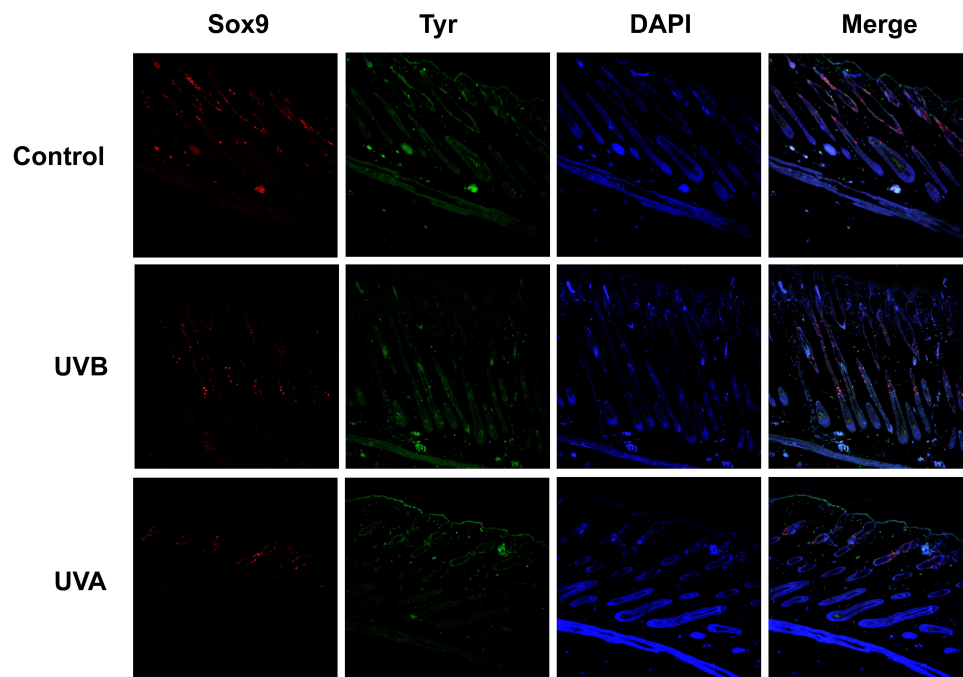


Figure 8 Red fluorescence was labelled for Sox9 as a marker for HFSCs. Tyr-positive cells labelled by green fluorescence were located in the hair bulbs and epidermis. HFSCs and melanocytes were decreased as shown by the merged images in the UVA group. There was an increase of Tyr-positive cells in the epidermis of the UVA group.

change in Fos expression was observed only in the UVB group. The relationship between phenotypes of photoaging and tumor susceptibility need further study.

Conclusion

UVA caused the decrease of HFSCs, TA cells, and melanocytes, resulting in hair follicle photoaging

characterized by the miniaturization of hair follicles and the increase of gray hair. UVA was an ideal light source for establishing a B57BL/6J mouse hair follicle photoaging model. UV up-regulated the expression of the Wnt signaling pathway in hair follicles, which may obviously prolong the hair follicle cycle in the UVB group.

Acknowledgments

This study was supported by the National Natural Science Foundation of China (NO. 81771994).

Disclosure

The authors report no conflicts of interest in this work.

References

- Park A, Khan S, Rawnsley J. Hair biology: growth and pigmentation. *Facial Plastic Surg Clin N Am*. 2018;26(4):415–424. doi:10.1016/j.fsc.2018.06.003
- Alonso L, Fuchs E. The hair cycle. *J Cell Sci*. 2006;119:391–393. doi:10.1242/jcs.02793
- Van Mater D, Kolligs F, Dlugosz A, Fearon E. Transient activation of beta-catenin signaling in cutaneous keratinocytes is sufficient to trigger the active growth phase of the hair cycle in mice. *Genes Develop*. 2003;17(10):1219–1224. doi:10.1101/gad.1076103
- Rabbani P, Takeo M, Chou W, et al. Coordinated activation of Wnt in epithelial and melanocyte stem cells initiates pigmented hair regeneration. *Cell*. 2011;145(6):941–955. doi:10.1016/j.cell.2011.05.004
- Plikus M, Mayer J, de la Cruz D, et al. Cyclic dermal BMP signalling regulates stem cell activation during hair regeneration. *Nature*. 2008;451(7176):340–344. doi:10.1038/nature06457
- Puizina-Ivić N. Skin aging. *Acta Dermatovenerol Alp Pannonica Adriat*. 2008;17(2):47–54.
- Gilchrest B. Photoaging. *J Invest Dermatol*. 2013;133:E132–136. doi:10.1038/skinbio.2013.176
- Fisher G, Kang S, Varani J, et al. Mechanisms of photoaging and chronological skin aging. *Arch Dermatol*. 2002;138(11):1462–1470. doi:10.1001/archderm.138.11.1462
- Kim J, Kim S, Noh E, et al. Reversine inhibits MMP-1 and MMP-3 expressions by suppressing of ROS/MAPK/AP-1 activation in UV-stimulated human keratinocytes and dermal fibroblasts. *Exp Dermatol*. 2018;27(3):298–301. doi:10.1111/exd.13494
- Gong M, Zhang P, Li C, Ma X, Yang D. Protective mechanism of adipose-derived stem cells in remodelling of the skin stem cell niche during photoaging. *Cellular Physiol Biochem*. 2018;51(5):2456–2471. doi:10.1159/000495902
- Kurdykowski S, Mine S, Bardey V, et al. Ultraviolet-B irradiation induces epidermal up-regulation of heparanase expression and activity. *J Photochem Photobiol B Biol*. 2012;106:107–112. doi:10.1016/j.jphotobiol.2011.10.013
- Hernández A, Vallejo B, Ruzgas T, Björklund S. The effect of UVB irradiation and oxidative stress on the skin barrier—a new method to evaluate sun protection factor based on electrical impedance spectroscopy. *Sensors*. 2019;19(10):2376. doi:10.3390/s19102376
- Chiu H, Chen C, Chen Y, Hsu Y. Far-infrared suppresses skin photoaging in ultraviolet B-exposed fibroblasts and hairless mice. *PLoS One*. 2017;12(3):e0174042. doi:10.1371/journal.pone.0174042
- Blanpain C, Fuchs E. Epidermal homeostasis: a balancing act of stem cells in the skin. *Nature Rev Mol Cell Biol*. 2009;10(3):207–217. doi:10.1038/nrm2636
- Myers R, Hamilton J. Regeneration and rate of growth of hairs in man. *Ann New York Acad Sci*. 1951;53(3):562–568. doi:10.1111/j.1749-6632.1951.tb31957.x
- Jahoda C, Whitehouse J, Reynolds A, Hole N. Hair follicle dermal cells differentiate into adipogenic and osteogenic lineages. *Exp Dermatol*. 2003;12(6):849–859. doi:10.1111/j.0906-6705.2003.00161.x
- Rufaut N, Goldthorpe N, Wildermoth J, Wallace O. Myogenic differentiation of dermal papilla cells from bovine skin. *J Cell Physiol*. 2006;209(3):959–966. doi:10.1002/jcp.20798
- Lako M, Armstrong L, Cairns P, Harris S, Hole N, Jahoda C. Hair follicle dermal cells repopulate the mouse haematopoietic system. *J Cell Sci*. 2002;115:3967–3974. doi:10.1242/jcs.00060
- Amoh Y, Li L, Katsuoka K, Penman S, Hoffman R. Multipotent nestin-positive, keratin-negative hair-follicle bulge stem cells can form neurons. *Proc Natl Acad Sci USA*. 2005;102(15):5530–5534. doi:10.1073/pnas.0501263102
- Amoh Y, Li L, Campillo R, et al. Implanted hair follicle stem cells form Schwann cells that support repair of severed peripheral nerves. *Proc Natl Acad Sci USA*. 2005;102(49):17734–17738. doi:10.1073/pnas.0508440102
- Liu J, Zhao K, Feng Z, Qi F. Hair follicle units promote re-epithelialization in chronic cutaneous wounds: a clinical case series study. *Experimental Ther Med*. 2015;10(1):25–30. doi:10.3892/etm.2015.2465
- Lee J, Kang S, Lilja K, et al. Signalling couples hair follicle stem cell quiescence with reduced histone H3 K4/K9/K27me3 for proper tissue homeostasis. *Nature Commun*. 2016;7:11278. doi:10.1038/ncomms11278
- White A, Khuu J, Dang C, et al. Stem cell quiescence acts as a tumour suppressor in squamous tumours. *Nature Cell Biol*. 2014;16(1):99–107. doi:10.1038/ncb2889
- Vidal Y, Chaboissier M, Lützkendorf S, et al. Sox9 is essential for outer root sheath differentiation and the formation of the hair stem cell compartment. *Curr Biol*. 2005;15(15):1340–1351. doi:10.1016/j.cub.2005.06.064
- Myung P, Takeo M, Ito M, Atit R. Epithelial Wnt ligand secretion is required for adult hair follicle growth and regeneration. *J Invest Dermatol*. 2013;133(1):31–41. doi:10.1038/jid.2012.230
- Wu P, Zhang Y, Xing Y, et al. The balance of Bmp6 and Wnt10b regulates the telogen-anagen transition of hair follicles. *Cell Commun Signal*. 2019;17(1):16. doi:10.1186/s12964-019-0330-x
- Lu Z, Xie Y, Huang H, et al. Hair follicle stem cells regulate retinoid metabolism to maintain the self-renewal niche for melanocyte stem cells. *eLife*. 2020;9:e52712. doi:10.7554/eLife.52712
- Suen W, Li S, Hes YL. 1 regulates anagen initiation and hair follicle regeneration through modulation of hedgehog signaling. *Stem Cells*. 2020;38(2):301–314. doi:10.1002/stem.3117
- Sokol S. Maintaining embryonic stem cell pluripotency with Wnt signaling. *Development*. 2011;138(20):4341–4350. doi:10.1242/dev.066209
- Yamada T, Hasegawa S, Inoue Y, et al. Wnt/β-catenin and kit signaling sequentially regulate melanocyte stem cell differentiation in UVB-induced epidermal pigmentation. *J Invest Dermatol*. 2013;133(12):2753–2762. doi:10.1038/jid.2013.235
- Assarsson M, Söderman J, Duvetorp A, Mrowietz U, Skarstedt M, Seifert O. Narrowband UVB treatment induces expression of WNT7B, WNT10B and TCF7L2 in psoriasis skin. *Arch Dermatol Res*. 2019;311(7):535–544. doi:10.1007/s00403-019-01931-y
- Lu Z, Fischer T, Hasse S, et al. Profiling the response of human hair follicles to ultraviolet radiation. *J Invest Dermatol*. 2009;129(7):1790–1804. doi:10.1038/jid.2008.418

33. de Lacharrière O, Deloche C, Misciali C, et al. Hair diameter diversity: a clinical sign reflecting the follicle miniaturization. *Arch Dermatol.* 2001;137(5):641–646.
34. Mai W, Sun Y, Liu X, Lin D, Lu D. Characteristic findings by phototrichogram in southern Chinese women with Female pattern hair loss. *Skin Res Technol.* 2019;25(4):447–455. doi:10.1111/srt.12672
35. Sachs D, Varani J, Chubb H, et al. Atrophic and hypertrophic photoaging: clinical, histologic, and molecular features of 2 distinct phenotypes of photoaged skin. *J Am Acad Dermatol.* 2019;81(2):480–488. doi:10.1016/j.jaad.2019.03.081
36. Guinea-Viniegra J, Zenz R, Scheuch H, et al. Differentiation-induced skin cancer suppression by FOS, p53, and TACE/ADAM17. *J Clin Invest.* 2012;122(8):2898–2910. doi:10.1172/JCI63103
37. Karnik P, Shah S, Dvorkin-Wininger Y, Oshtory S, Mirmirani P. Microarray analysis of androgenetic and senescent alopecia: comparison of gene expression shows two distinct profiles. *J Dermatol Sci.* 2013;72(2):183–186. doi:10.1016/j.jdermsci.2013.06.017

Clinical, Cosmetic and Investigational Dermatology

Dovepress

Publish your work in this journal

Clinical, Cosmetic and Investigational Dermatology is an international, peer-reviewed, open access, online journal that focuses on the latest clinical and experimental research in all aspects of skin disease and cosmetic interventions. This journal is indexed on CAS.

The manuscript management system is completely online and includes a very quick and fair peer-review system, which is all easy to use. Visit <http://www.dovepress.com/testimonials.php> to read real quotes from published authors.

Submit your manuscript here: <https://www.dovepress.com/clinical-cosmetic-and-investigational-dermatology-journal>